

Measurement of background gas in paraffin-coated alkali vapor cells

Naota Sekiguchi, Atsushi Hatakeyama

Department of Applied Physics, Tokyo University of Agriculture and Technology, Koganei, Tokyo 184-8588, Japan
 e-mail: hatakeya@cc.tuat.ac.jp
 Tel: +81 (0) 42 388 7554
 Fax: +81 (0) 42 388 7554

February 17, 2019

Abstract We measured the rate of velocity-changing collisions (VCCs) between alkali atoms and background gas in buffer-gas-free anti-spin-relaxation-coated cells. The average VCC rate in paraffin-coated rubidium vapor cells prepared in this work was $1 \times 10^6 \text{ s}^{-1}$, which corresponds to $\sim 1 \text{ mm}$ in the mean free path of rubidium atoms. This short mean free path indicates that alkali atoms do not travel freely between the cell walls. In addition, we found that a heating process known as “ripening” increases the VCC rate, and also confirmed that ripening improves the anti-relaxation performance of the coatings.

1 Introduction

There are two major techniques used to preserve a spin-polarized ground state of alkali atoms in a glass cell. The first is to fill the cell with an inert buffer gas. The second is to cover the inner glass surfaces with a so-called anti-relaxation coating. The interaction of the anti-relaxation coating with alkali atoms is much weaker than that of the bare glass surface, which causes the alkali atoms to bounce many times without relaxation of spin polarization. Paraffin, the best known anti-relaxation coating material, can bounce alkali atoms up to 10 000 times before wall-induced relaxation [1, 2]. Buffer-gas-free anti-relaxation-coated cells have a number of advantages over buffer-gas cells: the broadening of magnetic resonance lines due to field inhomogeneity can be reduced because alkali atoms sample the entire volume of the cell, and also it is possible to polarize and detect alkali atoms more effectively because there is no pressure broadening of the optical resonance line. Buffer-gas-free anti-relaxation-coated cells have therefore been used in many applications, including atomic clocks [3, 4], ultra-sensitive magnetometry [5–7], quantum memory [8], and studies of light propagation [9]. In these experiments, the background gas pressure is thought to be low enough to ignore collisions between alkali atoms and the background gas. However, the high reactivity of alkali atoms would lead to the generation of additional gases

by chemical reactions. Are the coated cells really “buffer-gas-free” in the sense that alkali atoms travel freely between the walls?

In fact, chemical reactions with silicon compound coatings and resulting outgassing have been reported [10–13]. If the background gas pressure is too high for alkali atoms to travel freely between the walls, the influences of the collisions should be taken into account. For example, collisions between cesium atoms and hydrogen molecules, which are typical species of the background gas [10–12], shift the ground state hyperfine transition frequency by 14 Hz/Pa [14] at 30°C and may be problematic in atomic clock applications. However, background gas pressures in buffer-gas-free cells have not been reported except for a very high pressure ($\leq 600 \text{ Pa}$) background gas in a microfabricated cell with an octadecyltrichlorosilane coating [15].

In situ pressure measurement without breaking the cell makes it possible to track the history of the pressure over the heating process, sometimes called “ripening,” which may accelerate chemical reactions. Ripening is generally performed on coated cells before experiments to increase alkali vapor density [2, 10, 16–18], because the initial alkali vapor density is much lower than its saturation vapor density. It has been reported that ripening improves anti-relaxation performance [10, 18], although there are concerns that ripening may simply reduce the collision rate of atoms with the cell surface by increasing the background gas pressure [10].

Here, we report a simple and effective method for measuring the rate of velocity-changing collisions (VCCs) between alkali atoms and background gas without breaking the cell when the gas pressure is low enough not to cause pressure broadening. The background gas pressure and mean free path of alkali atoms can be estimated from the measured VCC rate. This measurement was demonstrated in rubidium (Rb) vapor cells with a paraffin coating. We found that the VCC rates were higher than a few 10^5 s^{-1} . The mean free path of Rb atoms and the background gas pressure were estimated to be a few mm and several Pa, respectively. In addition, by measuring the VCC rates before and after ripening, we found that ripening increased the background gas pressure.

The spin-relaxation times were also measured before and after ripening, and the number of bounces before relaxation was evaluated. We found that ripening increased the number of bounces.

2 VCC-rate measurement

2.1 Method

Our method to measure the VCC rate γ is based on velocity-selective optical pumping and VCC-induced redistribution of the velocity of spin-polarized alkali atoms. A resonant, circularly polarized pump laser pulse selectively polarizes alkali atoms whose velocity components v_z along the laser propagation direction lie within a narrow velocity distribution centered at $v_z = 0$. The pump pulse irradiates alkali atoms for only a short duration. Spin polarization is detected with a counterpropagating collinear probe laser beam (see Fig. 1a). The diameter of the probe beam is much larger than that of the pump beam. The probed signal $S(t)$ decreases with time t due to two different mechanisms. First, the ballistic escape of the polarized atoms from the probe beam region decreases $S(t)$. Second, the VCCs between alkali atoms and the background gas causes a decrease in $S(t)$, as the VCCs redistribute the atomic velocity of the polarized atoms toward the Maxwell-Boltzmann distribution, resulting in fewer atoms within a probed velocity range (Fig. 1b). The signal $S(t)$ is thus described by

$$S(t) \propto S_{\text{esc}}(t) \times S_c(t), \quad (1)$$

where the contributions of the ballistic escape and the VCCs are denoted as $S_{\text{esc}}(t)$ and $S_c(t)$, respectively. Detailed discussions about $S_{\text{esc}}(t)$ and $S_c(t)$ will be provided in Sec. 2.3.

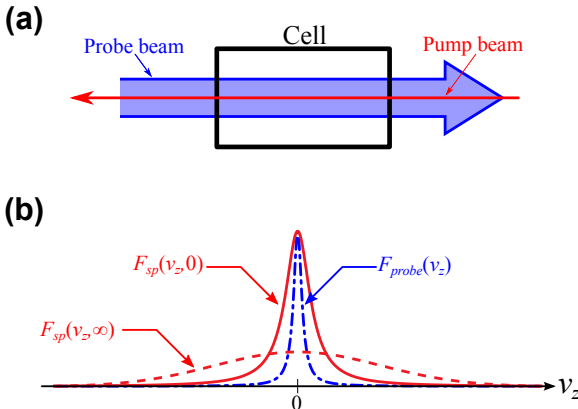


Fig. 1 (Color online) Schematic illustration of VCC rate measurement. (a) Spin polarization produced by the pump pulse is detected with the probe beam, which is counterpropagating and collinear to the pump beam. (b) The probe beam detects the spin polarization of atoms within the velocity distribution $F_{\text{probe}}(v_z)$. The initial velocity distribution $F_{\text{sp}}(v_z, 0)$ of spin polarization is redistributed toward $F_{\text{sp}}(v_z, \infty)$.

2.2 Experimental setup

Measurement of the VCC rate was carried out for paraffin-coated Rb vapor cells, the fabrication procedure of which will be described in Sec. 3. A longitudinal magnetic field of 40 μT was applied to the vapor cell with Helmholtz coils in a permalloy magnetic shield. The frequencies of the pump and the probe beams were stabilized to the $F = 3 \rightarrow F' = 4$ transition frequency of the ^{85}Rb $D2$ line. The profiles of the beams were measured with a CMOS camera and fitted by Gaussian functions. The diameters of the probe and the pump beams at which their intensities were reduced by $1/e$ compared to the beam center intensity were 0.27 cm and 0.037 cm, respectively. The probe beam power was 10 μW , and the pump beam power was 0.3 mW. The pump beam irradiated the cell for 1 μs and was then shut off with an acousto-optic modulator at $t = 0$. Measurements were performed for the left- and right-circularly polarized probe beams, and the signal $S(t)$ was derived from the difference between the transmitted powers for the two polarizations.

2.3 Analysis

Experimental data for an uncoated cell and a paraffin-coated cell are shown in Fig. 2 by blue and red points, respectively. It is clear that the decrease in signal $S(t)$ for the paraffin-coated cell was more rapid than that for the uncoated cell. The paraffin-coated cell, therefore, contained more background gas than the uncoated cell. To derive the VCC rate, we simulated the signal $S(t)$ with the following model.

First, we considered the contribution $S_{\text{esc}}(t)$ of the ballistic escape to the signal $S(t)$. The polarized atoms' velocity component v_r perpendicular to the beams obeys the Maxwell-Boltzmann distribution. For simplicity, we assumed that the pump beam diameter was infinitely small and atoms were polarized at the center of the probe beam at $t = 0$. The probability $G(v_r)dv_r$ that a polarized atom has a velocity between v_r

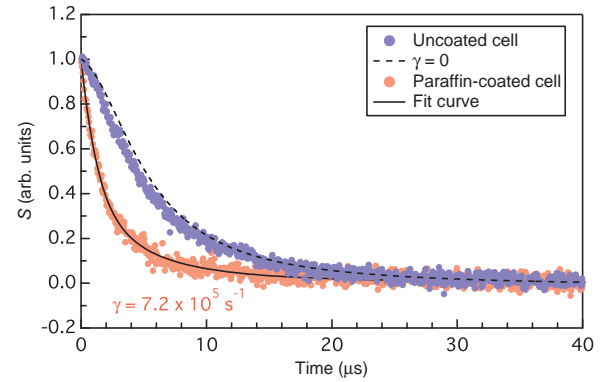


Fig. 2 (Color online) Signals S of the VCC rate measurement for an uncoated cell shown by blue points and a paraffin-coated cell (#2, post-ripening) shown by red points. Both data are normalized at 0 μs . The dashed line shows a simulation of the S without VCCs. The solid line shows a fit curve to the data for the coated cell.

and $v_r + dv_r$ was yielded as

$$G(v_r)dv_r = \frac{2v_r}{v_D^2} \exp \left\{ -\left(\frac{v_r}{v_D} \right)^2 \right\} dv_r, \quad (2)$$

where the most probable speed v_D is given by $v_D = \sqrt{2k_B T/m}$ with the Boltzmann constant k_B , the absolute temperature T , and the atomic mass m . The polarized atoms move at a constant velocity during the ballistic escape. Hence, the probability $\rho(r, t)dr$ that a polarized atom is at a distance from the center between r and $r + dr$ at time t was derived from Eq. (2) as

$$\rho(r, t)dr = \frac{2r}{(v_D t)^2} \exp \left\{ -\left(\frac{r}{v_D t} \right)^2 \right\} dr. \quad (3)$$

The signal is proportional to the intensity of the probe beam at the position of a polarized atom:

$$S_{esc}(t) \propto \int_0^\infty I_{probe}(r) \times \rho(r, t)dr. \quad (4)$$

Here, the beam profile $I_{probe}(r)$ of the probe beam was described by a Gaussian function

$$I_{probe}(r) \propto \exp \left\{ -\left(\frac{2r}{\phi_{probe}} \right)^2 \right\}, \quad (5)$$

where the probe beam diameter $\phi_{probe} = 0.27$ cm, as mentioned above. By substituting Eqs. (3), (5) into Eq. (4), $S_{esc}(t)$ was obtained as

$$S_{esc}(t) \propto \frac{1}{\phi_{probe}^2 + 4v_D^2 t^2}. \quad (6)$$

Next, we considered the contribution $S_c(t)$ of the VCCs to the signal $S(t)$. The velocities of the polarized alkali atoms are changed due to the VCCs, while the polarization is preserved. The velocity distribution of the spin polarization, therefore, depends on t and is described as $F_{sp}(v_z, t)$. The pump pulse beam produces the initial Lorentzian distribution $F_{sp}(v_z, t = 0)$, which corresponds to the absorption profile for the pump laser. In the steady state, $F_{sp}(v_z, t = \infty)$ should be proportional to the Maxwell-Boltzmann distribution. The probe beam detects the polarization within the velocity distribution $F_{probe}(v_z)$, which is proportional to the absorption cross-section for the probe beam. The signal detected with the probe beam is proportional to the integral of the product of $F_{sp}(v_z, t)$ and $F_{probe}(v_z)$ over the velocity v_z ,

$$S_c(t) \propto \int_{-\infty}^\infty F_{sp}(v_z, t) \times F_{probe}(v_z) dv_z. \quad (7)$$

We assumed the time variation of $F_{sp}(v_z, t)$ as

$$\frac{\partial F_{sp}(v_z, t)}{\partial t} = -\gamma [F_{sp}(v_z, t) - F_{sp}(v_z, \infty)], \quad (8)$$

where the steady-state velocity distribution $F_{sp}(v_z, \infty)$ was given by

$$F_{sp}(v_z, \infty) = \int_{-\infty}^\infty F_{sp}(v'_z, 0) dv'_z \times \frac{1}{v_D \sqrt{\pi}} \exp \left\{ -\left(\frac{v'_z}{v_D} \right)^2 \right\}. \quad (9)$$

We then calculated $S_c(t)$ from Eqs. (7), (8), and (9).

As the pump pulse has a finite duration $\tau = 1$ μ s, the experimental data were compared with $\int_{-\tau}^0 S_{esc}(t-t') \times S_c(t-t') dt'$. The curve calculated with the VCC rate $\gamma = 0$ (the dashed line in Fig. 2) in the absence of VCCs is in reasonable agreement with the experimental data for the uncoated cell. The experimental data for the coated cell were well fitted by the curve with $\gamma = 7.2 \times 10^5$ s^{-1} (the solid line in Fig. 2).

2.4 Estimation of background gas pressure and mean free path of alkali atoms

The VCC rate γ is given by $\gamma = n\sigma_c \bar{v}$. Here, n is the number density of background gas, σ_c is the cross-section of VCCs, and \bar{v} is the mean relative velocity. The mean free path λ of Rb atoms is then $\lambda = 1/(n\sigma_c) = \bar{v}/\gamma$. Although the background gas species were unknown in this work, we assumed $\bar{v} = 1 \times 10^5$ cm/s as most components of the background gas in some silicon compound-coated cells are light [10–12]. From the ideal gas law, the pressure p of the background gas was estimated by $p = k_B T/(\lambda\sigma_c)$, where σ_c was assumed to be $\sigma_c = 1 \times 10^{-14}$ cm² by reference to Ref. 19 regarding Na-Ne collisions. The mean free path and background gas pressure for the paraffin-coated cell shown in Fig. 2 were estimated to be 1.4 mm and 3.0 Pa, respectively.

3 Cell preparation and spin-relaxation measurement

The above evaluations were performed for seven paraffin-coated cells made of Pyrex glass. The dimensions of the coated cells are shown in Table 1. Each cell had a stem with a constricted capillary with a diameter of ~ 1 mm to be connected to a vacuum system. The coating procedure was similar to those reported previously [16, 17]. Coating material was fractional distilled between 220°C and 240°C from commercial paraffin wax Sasolwax® H1 produced by Sasol Wax. The cell was evacuated below 10⁻⁴ Pa with a turbomolecular pump and baked at 420°C for 4 hours. After deposition of paraffin at 380°C or 400°C, the cell was re-evacuated below 10⁻⁴ Pa and then sealed with Rb metal (in natural isotopic abundance) at the stem. In this work, initial Rb vapor density was sufficiently high to carry out the VCC rate and spin-relaxation

Table 1 Characteristics of cylindrical paraffin-coated cells. The coated cells are numbered from #1 to #7.

Cell	Diameter (mm)	Length (mm)	τ_s (s)	
			Pre-ripening	Post-ripening
#1	17.0	24.4	0.15	0.18
#2	17.0	27.2	0.046	0.082
#3	17.0	27.4	0.037	0.15
#4	17.0	25.0	0.040	0.19
#5	17.0	24.3	0.17	0.22
#6	17.0	23.7	0.22	0.24
#7	17.0	24.3	0.081	0.13

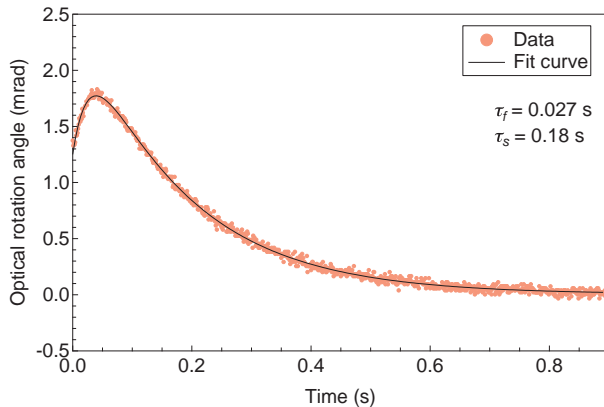


Fig. 3 (Color online) Spin relaxation time measurement in a paraffin-coated cell (# 1, post-ripening). The experimental data were fitted by a double exponential function.

time measurements. The measurements were also performed after ripening, during which the cell was heated at 80°C for 10 hours while the stem was kept at 75°C.

The longitudinal spin-relaxation times of the fabricated cells were measured in a manner similar to that described previously [18]. The cell was placed in the magnetic shield and immersed in a longitudinal magnetic field of 40 μ T. A circularly polarized laser light (pump light) produced spin polarization of Rb atoms and was shut off at time $t = 0$. A linearly polarized laser light (probe light) and a balanced polarimeter detected the optical rotation induced by spin polarization. The power of the probe light was 5 μ W, and the probe beam profile was the same as that used in VCC-rate measurement. Figure 3 shows the time dependence of the optical rotation angle in a paraffin-coated cell (# 1, post-ripening). The angle of the polarization plane of the probe light for the unpolarized atoms was adjusted to 0.0 mrad. The data were fitted by a double exponential function and indicated two relaxation components, a fast relaxation time τ_f and a slow relaxation time τ_s , with opposite signs as reported previously [18]. We focused on the slow relaxation time τ_s , which is shown in Table 1.

4 Results and Discussion

VCC rates in all prepared coated cells are shown in Fig. 4. Although there was variation in VCC rate among the coated cells, VCC rates in the post-ripening coated cells were increased to higher than a few 10^5 s^{-1} . The corresponding mean free paths were shorter than a few mm, which was much smaller than the dimensions of a typical cell. It is clear that the ripening process made the background gas pressure higher in all coated cells.

To test the generality of our results, we also measured the VCC rate in a pwMB-coated cell fabricated in a different laboratory. The coating material pwMB was mentioned in Refs. 17,20,21. The pwMB-coated cell was spherical (47 mm in diameter) and filled with enriched ^{85}Rb . The VCC rate in

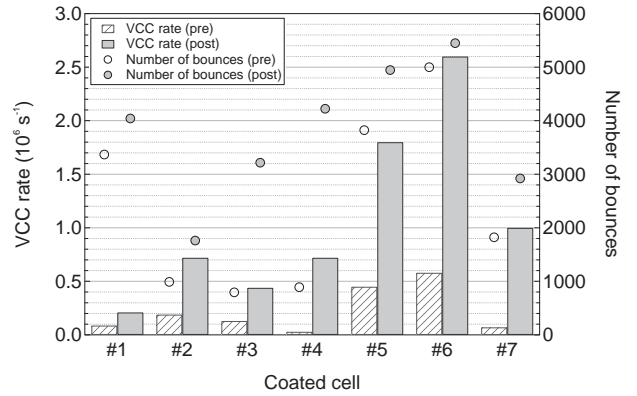


Fig. 4 VCC rates (left axis) and number of bounces (right axis) for pre- and post-ripening coated cells. Hatched bars show VCC rates for pre-ripening cells, and gray bars show those for post-ripening cells. The numbers of bounces for pre- and post-ripening cells are shown by open circles and gray circles, respectively.

the pwMB-coated cell was measured as $3.8 \times 10^5 \text{ s}^{-1}$. The mean free path and the background gas pressure were estimated to be 2.6 mm and 1.6 Pa, respectively. It is therefore very likely that paraffin-coated cells generally have relatively high background gas pressures.

With the VCC rates in mind, we evaluated the number of bounces N before depolarization under the assumption that Rb atoms moved diffusively as described previously [22]. In the evaluation, the diffusion coefficient D had two variations. One was estimated from the classical diffusion coefficient $D = \lambda v_m/3$, where the mean speed v_m of Rb atoms is given by $v_m = 2v_D/\sqrt{\pi}$. The other was estimated from the diffusion coefficient for Rb atoms in hydrogen molecules [23] and the estimated background gas pressure. In addition, the number of bounces in the absence of VCCs was also calculated by

$$N = \frac{v_m A}{4V} \times \tau_s. \quad (10)$$

Here, A is the inner surface area and V is the volume of the cell. The numbers evaluated in these three ways were almost the same and are shown in Fig. 4. It is clear that the number of bounces, i.e., the anti-relaxation performance of the coating, was improved by ripening.

5 Conclusions

We measured the rates of VCCs between Rb atoms and background gas in seven buffer-gas-free, paraffin-coated cells. The results indicated an average VCC rate of $1 \times 10^6 \text{ s}^{-1}$. This VCC rate corresponds to the mean free path of 1 mm and the background gas pressure of 4 Pa. This short mean free path compared to the cell dimensions means that Rb atoms in the coated cells do not travel freely between the cell walls. We also found that the so-called “ripening” process increased the background gas pressure. We confirmed improvement of the anti-relaxation performance of the paraffin coatings by

ripening. The relatively high VCC rates indicated that precise experiments using coated cells require attention to the effects induced by collisions with background gas. In particular, the background gas pressure should be checked when coated cells are heated.

Acknowledgements We would like to thank Mikhail V. Balabas for fabrication of the pwMB-coated cell and for his helpful comments, and Antoine Weis for his important advice. This work was supported by a Grant-in-Aid for Scientific Research (No. 23244082) from the Japan Society for the Promotion of Science (JSPS).

References

1. H.G. Robinson, E.S. Enberg, and H.G. Dehmelt, *Bull. Am. Phys. Soc.* **3**, 9 (1958)
2. M.A. Bouchiat and J. Brossel, *Phys. Rev.* **147**, 41 (1966)
3. H.G. Robinson and C.E. Johnson, *Appl. Phys. Lett.* **40**, 771 (1982)
4. T. Bandi, C. Affolderbach, and G. Milet, *J. Appl. Phys.* **111**, 124906 (2012)
5. J. Dupont-Roc, S. Haroche, and C. Cohen-Tannoudji, *Phys. Lett. A* **28**, 638 (1969)
6. D. Budker, D.F. Kimball, S.M. Rochester, V.V. Yashchuk, and M. Zolotorev, *Phys. Rev. A* **62**, 043403 (2000)
7. D. Budker and M. Romalis, *Nat. Phys.* **3**, 227 (2007)
8. B. Julsgaard, J. Sherson, J.I. Cirac, J. Fiurasek, and E.S. Polzik, *Nature* **432**, 482 (2004)
9. D. Budker, D. F. Kimball, S.M. Rochester, and V.V. Yashchuk, *Phys. Rev. Lett.* **83**, 1767 (1999)
10. J.C. Camparo, R.P. Frueholz, and B. Jaduszliwer, *J. Appl. Phys.* **62**, 676 (1987)
11. Y.W. Yi, H.G. Robinson, S. Knappe, J.E. MacLennan, C.D. Jones, C. Zhu, N.A. Clark, and J. Kitching, *J. Appl. Phys.* **104**, 023534 (2008)
12. S.N. Atutov, R. Calabrese, A.I. Plekhanov, and L. Tomassetti, *Eur. Phys. J. D* **68**, 6 (2014)
13. M. Stephens, R. Rhodes, and C. Wieman, *J. Appl. Phys.* **76**, 3479 (1994)
14. M. Arditi and T.R. Carver, *Phys. Rev.* **112**, 449 (1958)
15. R. Straessle, M. Pellaton, C. Affolderbach, Y. Pétremand, D. Briand, G. Milet, and N.F. de Rooij, *Appl. Phys. Lett.* **105**, 043502 (2014)
16. E.B. Alexandrov, M.V. Balabas, D. Budker, D. English, D.F. Kimball, C.-H. Li, and V.V. Yashchuk, *Phys. Rev. A* **66**, 042903 (2002)
17. S.J. Seltzer, M.-A. Bouchiat, and M.V. Balabas, in *Optical Magnetometry*, edited by D. Budker and D.F.J. Kimball, (Cambridge University Press, Cambridge, 2013) pp. 205–224
18. M.T. Graf, D.F. Kimball, S.M. Rochester, K. Kerner, C. Wong, D. Budker, E.B. Alexandrov, M.V. Balabas, and V.V. Yashchuk, *Phys. Rev. A* **72**, 023401 (2005)
19. C.G. Aminoff, J. Javanainen, and M. Kaivola, *Phys. Rev. A* **28**, 722 (1983)
20. S.J. Seltzer, D.J. Michalak, M.H. Donaldson, M.V. Balabas, S.K. Barber, S.L. Bernasek, M.-A. Bouchiat, A. Hexemer, A.M. Hibberd, D.F.J. Kimball, C. Jaye, T. Karaulanov, F.A. Narducci, S.A. Rangwala, H.G. Robinson, A.K. Shmakov, D.L. Voronov, V.V. Yashchuk, A. Pines, and D. Budker, *J. Chem. Phys.* **133**, 144703 (2010)
21. A.M. Hibberd, S.J. Seltzer, M.V. Balabas, M. Morse, D. Budker, and S.L. Bernasek, *J. Appl. Phys.* **114**, 094513 (2013)
22. S.J. Seltzer, D.M. Rampulla, S. Rivillon-Amy, Y.J. Chabal, S.L. Bernasek, and M.V. Romalis, *J. Appl. Phys.* **104**, 103116 (2008)
23. R.J. McNeal, *J. Chem. Phys.* **37**, 2726 (1962)